

# Ferroelectric, ferrielectric and antiferroelectric mesophases in compounds with a polybenzyloxycarbonyl mesogenic core

Ewa Dzik, Józef Mieczkowski,\* Ewa Gorecka and Damian Pocięcha

Received 9th November 2004, Accepted 20th December 2004

First published as an Advance Article on the web 26th January 2005

DOI: 10.1039/b417144f

It was found that the synclinc interlayer interactions for materials having mesogenic cores made of repeating benzyloxycarbonyl units are stronger than for the parent MHPOBC and analogous compounds having biphenyl–phenyl mesogenic cores, as evidenced by significantly broader range of the synclinc phase and less frequent appearance of anticlinc phases in the homologous series. The biaxiality of the three-layer structure of the  $\text{SmC}^*_{\text{F11}}$  phase was directly observed at the temperature where the optical pitch is spontaneously unwound. The ferrielectric phase structure is nearly Ising-like. The Ising structure is most probably enforced by strong interlayer quadrupole order, in materials in which the ferri-phase appears nearly 20 K below the  $\text{SmA}$  phase.

## Introduction

Although more than 10 years have passed since the discovery of smectic  $\text{C}^*$  subphases<sup>1</sup> it is still not clear what kind of molecular interactions prompt the interlayer order. The vast majority, thousands of materials, form a synclinc  $\text{SmC}^*$  phase, while anticlinc order, leading to antiferroelectric properties for enantiomeric materials, is observed only in about 400 compounds. Most of them have branched terminal chains and a three-ring mesogenic core.<sup>2</sup> In some of these systems other tilted subphases,  $\text{SmC}^*_{\alpha}$ ,  $\text{SmC}^*_{\text{F11}}$  (described also as  $\text{SmC}^*_{\gamma}$  or  $\text{SmC}^*_{1/3}$ ) and  $\text{SmC}^*_{\text{F12}}$  (described also as  $\text{SmC}^*_{\text{AF}}$  or  $\text{SmC}^*_{1/4}$ ), also appear. They are observed only in chiral systems, in the temperature range where the synclinc and anticlinc interactions are almost equal.<sup>3</sup> It took nearly 10 years of intensive research to recognize the structure of these phases. The  $\text{SmC}^*_{\alpha}$  phase has a clock-like structure in which the director rotates by a constant azimuthal angle in the consecutive layers. The periodicity of this structure is from five to several smectic layers. The  $\text{SmC}^*_{\text{F11}}$  and  $\text{SmC}^*_{\text{F12}}$  phases have distorted clock-like structures with three and four layer periodicity, respectively.<sup>4</sup> It is believed that the structure of these phases is driven by the competition between synclinc or anticlinc nearest neighbour (NN) interactions and the anticlinc next nearest neighbour (NNN) interactions in systems with relatively strong NN quadrupole interactions<sup>5</sup> or thermal fluctuations that undulate the smectic layers.<sup>6</sup>

In smectic  $\text{SmC}^*_{\text{F11}}$  and  $\text{SmC}^*_{\text{F12}}$  phases apart from the chiral mesoscopic structure, defining the basic structural unit, long wavelength helical modulation also exists. It is still not clear how the chirality influences the unit structure of subphases and if and how the chirality is transferred in these phases between mesoscopic and macroscopic levels. For the  $\text{SmC}^*_{\text{F12}}$  phase it has been observed that the sign of the long wavelength helix may be reversed at certain temperatures although the handedness of the four layer structure is conserved.<sup>5</sup>

Most of the research on the  $\text{SmC}^*$  subphases has been done using compounds of the MnPOBC series,<sup>2</sup> that are homologues of the prototype antiferroelectric liquid crystal MHPOBC, or other materials having a biphenyl–phenyl core structure.<sup>7</sup> In this contribution we present the synthesis and characterization of a homologous series having a different mesogenic core consisting of repeating benzyloxycarbonyl units. In the studied materials either the chiral terminal chains were varied, or for fixed terminal chains different substituents, *i.e.* halogen atoms or  $\text{NO}_2$  groups, were attached laterally to the mesogenic core.

## Experimental

The mesophase identification was based on microscopic routine examination of the textures formed by samples between two glass plates. A Nikon Ophthot-2Pol polarising microscope equipped with a Mettler FP82HT hot stage was used. The differential scanning calorimetry measurements were performed using a Perkin Elmer DSC-7 calorimeter in the cooling and heating runs at scanning rates of 0.2–5  $\text{K min}^{-1}$ . For dielectric and electro-optic measurements, glass cells of various thicknesses (from 5 to 50  $\mu\text{m}$ ) with ITO or gold electrodes coated with polyimide were used. Dielectric spectroscopy studies were performed with an impedance analyzer (Solotron SI 1260) in the frequency window 1 Hz–10 MHz. The dielectric dispersion data were analyzed by fitting the temperature-dependent complex dielectric constant,  $\epsilon^*$ , to the Cole–Cole equation:

$$\epsilon^* - \epsilon_{\infty} = \frac{\Delta\epsilon}{1 + (if/f_r)^{1-\alpha}} + i \frac{\sigma}{2\pi\epsilon_0 f}$$

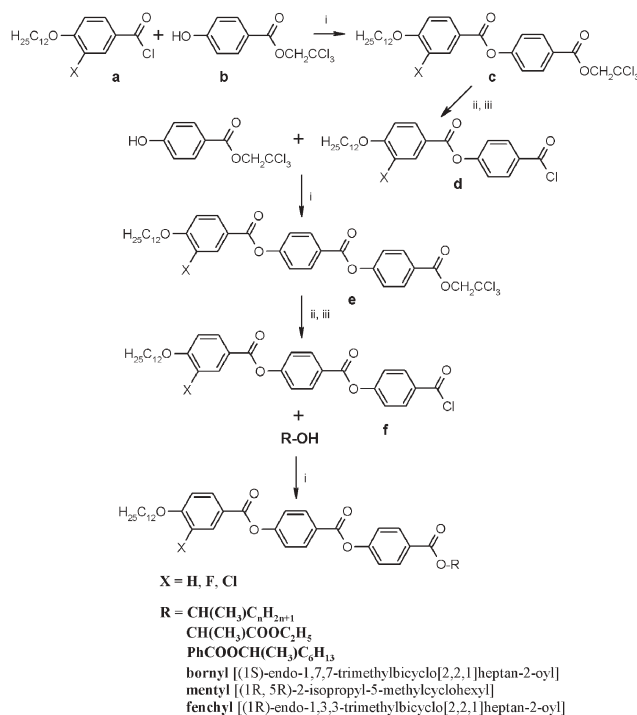
where  $\Delta\epsilon$ ,  $f_r$  and  $\alpha$  are the dielectric strength, relaxation frequency, and distribution parameter of the mode, respectively. For a single, Debye type relaxation the distribution parameter  $\alpha = 1$ . Spontaneous polarization was measured by integrating the switching current recorded during polarization reversal under applied triangular voltage. Tilt angle was measured in a planar cell placed between crossed polarizers,

\*mieczkow@chem.uw.edu.pl

by applying the opposite dc electric field and determining the angle difference between the minima of the light transmission positions. Optical rotatory power (ORP) was studied using a system consisting of a He–Ne laser, a photodiode (FLC PIN 20) and a lock-in amplifier (EG&G 7265), with 50–100  $\mu\text{m}$  thick free-standing film samples. The light transmission (LT) was recorded *versus* the angle between the polarizer and analyzer, the LT minimum was found by fitting LT to a square equation. The rotation angle, hence ORP, could be determined with an accuracy better than  $0.02^\circ$  in  $\text{SmC}^*_\text{A}$  and  $\text{SmC}^*_\text{C}$  phases, and  $\sim 0.1^\circ$  in  $\text{SmC}^*_\text{F11}$  phase, where considerable light scattering was observed upon approaching the helix inversion temperature. The selective reflection measurements were performed in transmission mode at normal incidence with a Shimadzu PC3101 spectrophotometer for free standing film samples in the wavelength range 200–3200 nm. At normal incidence the selective reflection from half pitch band was observed, at  $\lambda = np$ , the mean refractive index,  $n = 1.5$ , that is assumed to be temperature independent in the temperature range of measurements, was used for calculating the pitch length.

## Synthesis

The general synthesis procedure of the studied compounds is outlined in Schemes 1 and 2. The chiral substrates used in the synthesis were supplied by Aldrich ((*R*)-(-)-2-butanol: 99% ee/GLC, (*S*)-(+)-2-pentanol: 98% ee/GLC, (*R*)-(-)-2-heptanol: 95% ee/GLC, (*R*)-(-)-2-octanol: 98% ee/GLC, [(1*S*)-*endo*]-(-)-borneol: 98% ee/GLC, (1*R*,2*S*,5*R*)-(-)-menthol: 99% ee/GLC, (1*R*)-*endo*-(+)-fenchyl alcohol: 97% ee/GLC). To confirm the molecular structures of the synthesised compounds



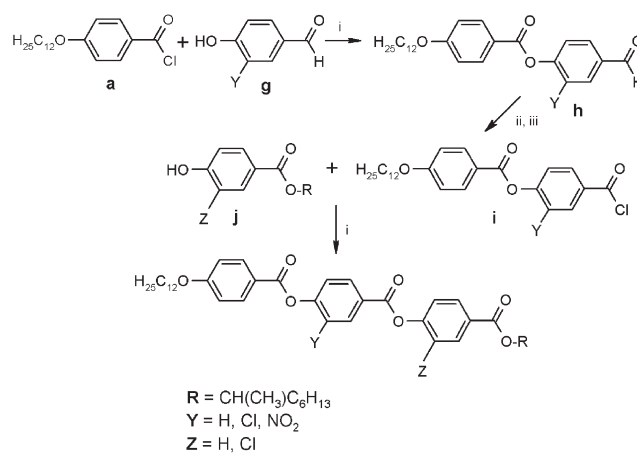
**Scheme 1** Reagents and conditions : i) TEA, THF, DMAP; ii) Zn/AcOH, THF; iii)  $(\text{COCl})_2$ , toluene, reflux.

some analytical methods were applied. Infrared (IR) spectra were obtained using a Nicolet Magna IR 500. The NMR spectra ( $^{13}\text{C}$ ) were recorded on a Varian Unity Plus spectrometer operating at 200 MHz, whereas  $^1\text{H}$  NMR spectra were recorded at 200 or 500 MHz when high signal separation was necessary. Tetramethylsilane was used as an internal standard. Chemical shifts are reported in ppm. TLC analyses were performed on Merck 60 silica gel plasticfolien and visualised using iodine vapour. Column chromatography was carried out at atmospheric pressure using silica gel (100–200 mesh, Merck). Composition of the synthesised compounds, determined by elemental analysis, confirmed the expected molecular structures.

**4-[(2,2,2-Trichloroethoxy)carbonyl]phenyl-4-dodecyloxybenzoate (c, X = H).** To 2,2,2-trichloroethyl 4-hydroxybenzoate **b** (2 g; 7.4 mmol) dissolved in dry THF (100 mL), TEA (10 mL), appropriate acid chloride **a** (X = H) (2.4 g; 7.4 mmol) in THF (100 mL) and 50 mg of DMAP were added. The mixture was refluxed with stirring during 6 h. The solvents were evaporated and the reaction mixture was chromatographed on silica gel using toluene as eluent. Compound **c** was obtained (2.56 g; 62% yield).

Elemental analysis for  $\text{C}_{28}\text{H}_{35}\text{O}_5\text{Cl}_3$ : Calc. C 60.27, H 6.28; Found C 60.20, H 6.32%;  $\nu_{\text{max}}$  (KBr)/ $\text{cm}^{-1}$  2920, 1730, 1610, 1290, 1030, 810, 690;  $\delta_{\text{H}}$  ( $\text{CDCl}_3$ ) 8.11–8.22 (m, 4H), 7.32–7.36 (m, 2H), 6.95–6.99 (m, 2H), 4.98 (s, 2H), 4.04 (t, 2H,  $J = 6.6$  Hz), 1.75–1.89 (m, 2H), 1.27 (s, 54H), 0.85–0.91 (m, 9H);  $\delta_{\text{C}}$  ( $\text{CDCl}_3$ ) 164.20, 163.84, 155.56, 132.42, 131.71, 126.02, 122.17, 120.87, 114.41, 95.04, 74.46, 68.37, 31.92, 29.64, 29.60, 29.56, 29.35, 29.08, 25.97, 22.70, 14.14.

**4-[[4-(2,2,2-Trichloroethoxycarbonyl)phenoxy]carbonyl]phenyl-4-dodecyloxybenzoate (e, X = H).** Ester **c** (2.0 g; 3.6 mmol), THF (100 mL), zinc dust (2.0 g; 30.7 mmol) and acetic acid (10 mL) were stirred at room temperature for 6 h. Zinc dust was filtered off and the filtrate was evaporated with toluene (100 mL). Remaining solid was washed with hexane and dried over phosphorus anhydride and was subsequently suspended in toluene (75 mL) to which oxalyl chloride (3.5 mL; 41.0 mmol) was added. The reaction mixture was heated for



**Scheme 2** Reagents and conditions : i) TEA, THF, DMAP; ii)  $\text{CrO}_3/\text{AcOH}$ ; iii)  $\text{SOCl}_2$ , toluene, reflux.

6 h at reflux. The precipitate was filtered off and the solvent was evaporated to dryness. The acid chloride **d** was obtained (1.4 g; 87%).

The acid chloride **d** (1.4 g; 3.1 mmol) dissolved in THF (25 mL) was added to the mixture of 2,2,2-trichloroethyl-4-hydroxybenzoate **b** (0.85 g; 3.1 mmol) in TEA (5 mL) and 50 mg of DMAP. The mixture was refluxed with stirring during 10 h. After evaporation of the solvents the product was purified with column chromatography on silica gel using toluene as eluent. Compound **e** was obtained (1.3 g; 62%).

Elemental analysis for  $C_{35}H_{39}Cl_3O_7$ : Calc. C 61.99, H 5.76; Found C 61.27, H 5.88%;  $\nu_{\max}$  (KBr)/ $cm^{-1}$  3040, 2910, 1750, 1610, 1450, 1260, 1040, 820, 710;  $\delta_H$  (CDCl<sub>3</sub>) 8.13–8.30 (m, 6H), 7.35–7.41 (m, 4H), 6.96–7.01 (m, 2H), 4.99 (s, 2H), 4.02–4.08 (m, 2H), 1.76–1.86 (m, 2H), 1.27 (s, 18H), 0.85–0.88 (m, 3H),  $\delta_C$  (CDCl<sub>3</sub>) 164.46, 164.34, 164.06, 155.87, 155.47, 132.62, 132.11, 131.99, 126.51, 126.45, 122.44, 122.30, 121.03, 114.63, 95.21, 74.69, 68.59, 32.11, 29.83, 29.78, 29.75, 29.55, 29.27, 26.17, 22.89, 14.33.

**4-[[4-((R)-2-Octyloxy)carbonyl]phenoxy]carbonyl]phenyl-4-dodecyloxybenzoate (compound 4).** To the ester **e** (1.3 g; 1.92 mmol) dissolved in THF (50 mL), zinc dust (1.3 g; 19.9 mmol) and acetic acid (10 mL) were added. The mixture was stirred at room temperature during 6 h. Zinc dust was filtered off, and the filtrate was evaporated with toluene (50 mL). The crude product was washed with hexane and dried over phosphorus anhydride. The obtained product was suspended in toluene (100 mL) and oxalyl chloride (2.5 mL, 29.5 mmol) was added. Reaction mixture were stirred and heated for 6 h at reflux. The precipitated solid was filtered and the filtrate evaporated to dryness. The acid chloride **f** was obtained (0.97 g; 90%). The acid chloride thus formed (0.97 g, 1.72 mmol), dissolved in THF (50 mL), was added to the mixture of (*R*)-(-)-2-octanol (0.21 mL, 1.38 mmol) in TEA (5 mL) and 50 mg of DMAP. The mixture was refluxed with stirring during 10 h. Then the solvents were evaporated and the product was purified *via* chromatography on silica gel eluting with toluene. Compound **4** was obtained (0.47 g; 52%).

Elemental analysis for  $C_{41}H_{54}O_7$ : Calc. C 74.77, H 8.21; Found C 74.89, H 8.32%;  $\nu_{\max}$  (KBr)/ $cm^{-1}$  3040, 2920, 2880, 1720, 1610, 1260, 1020, 830;  $\delta_H$  (CDCl<sub>3</sub>) 8.11–8.30 (m, 6H), 7.40–7.28 (m, 4H), 7.01–6.97 (m, 2H), 5.17 (sextet, 1H,  $J = 6.2$  Hz), 4.05 (t, 2H,  $J = 6.6$  Hz), 1.86–1.59 (m, 2H), 1.34 (d, 3H,  $J = 6.2$  Hz), 1.27 (s, 28H), 0.90–0.85 (m, 6H);  $\delta_C$  (CDCl<sub>3</sub>) 165.65, 164.51, 164.07, 155.80, 154.58, 132.64, 131.38, 128.84, 126.67, 122.40, 121.87, 121.08, 114.64, 72.17, 68.61, 36.28, 32.13, 31.95, 29.85, 29.80, 29.56, 29.37, 29.29, 26.18, 25.62, 22.90, 22.80, 20.31, 14.33, 14.28.

**2-Chloro-4-formylphenyl-4-(dodecyloxy)benzoate (h, Y = Cl).** To 3-chloro-4-hydroxybenzaldehyde (Y = Cl) (2 g; 13 mmol), dissolved in dry tetrahydrofuran (50 mL), was added TEA (10 mL), acid chloride **a** (5.1 g; 15.7 mmol) in THF (50 mL) and finally 50 mg of DMAP. Reaction mixture was refluxed with stirring during 10 h. The solvents were evaporated to dryness and crude products were separated by column chromatography with silica gel using toluene as eluent. Compound **h** was obtained (3.7 g; 65%).

Elemental analysis for  $C_{26}H_{33}ClO_4$ : Calc. C 70.19, H 7.42; Found C 70.11, H 7.47%;  $\nu_{\max}$  (KBr)/ $cm^{-1}$  3020, 2920, 2740, 1715, 1400, 1280, 1040, 820, 715;  $\delta_H$  (CDCl<sub>3</sub>) 10.02 (s, 1H), 8.12–8.17 (m, 3H), 7.94–7.99 (m, 1H), 7.32–7.41 (m, 1H), 6.96–7.01 (m, 2H), 4.05 (t, 2H,  $J = 6.1$  Hz), 1.76–1.89 (m, 2H), 1.27–1.43 (m, 18H), 0.88 (t, 3H,  $J = 6.2$  Hz),  $\delta_C$  (CDCl<sub>3</sub>) 191.00, 164.51, 163.34, 151.67, 136.29, 132.02, 131.21, 128.82, 127.59, 122.51, 118.45, 113.84, 68.40, 31.92, 29.64, 29.59, 29.55, 29.35, 29.08, 25.97, 22.69, 14.13.

**2-Chloro-4-(chlorocarbonyl)phenyl-4-dodecyloxybenzoate (i, Y = Cl).** To aldehyde **h** (2 g, 4.5 mmol), dissolved in concentrated acetic acid (100 mL), was added chromium(VI) oxide (0.9 g, 9.0 mmol) in 70% aqueous acetic acid (30 mL) and the mixture was stirred for 24 h at room temperature. Then the mixture was poured into water. The precipitated product was filtered and dried in a desiccator over phosphorus anhydride. The acid was purified by single crystallisation from methanol and had sufficient purity for the next step. To the acid in toluene (80 mL) was added thionyl chloride (1.5 mL, 20.5 mmol) and the reaction mixture was heated for 8 h at reflux. The solvents were evaporated to dryness. The acid chloride **i** was obtained (1.4 g, 65%).

**4-[(1-Methylheptyl)oxy]carbonyl]phenyl 3-chloro-4-[[4-(dodecyloxy)benzoyl]oxy]benzoate (compound 7).** To acid chloride **i** (0.46 g, 0.96 mmol), dissolved in dry THF (25 mL), was added (*R*)-2-octyl-4-hydroxybenzoate **j** (Z = H) (0.20 g; 0.8 mmol) in dry THF (25 mL), TEA (3 mL) and 50 mg of DMAP. The reaction mixture was refluxed with stirring during 10 h. After evaporation of the solvents the reaction mixture was chromatographed on silica gel using toluene as eluent. Compound **7** was obtained (0.32 g; 57.7%).

Elemental analysis for  $C_{41}H_{53}ClO_7$ : Calc. C 71.03, H 7.71; Found C 70.96, H 8.01%;  $\nu_{\max}$  (KBr)/ $cm^{-1}$  3040, 2930, 1710, 1620, 1300, 1030, 830, 70;  $\delta_H$  (CDCl<sub>3</sub>) 8.09–8.16 (m, 4H), 7.26–7.30 (d, 2H,  $J = 8.8$  Hz), 6.95–7.00 (d, 2H,  $J = 9.2$  Hz), 5.15 (sextet, 1H,  $J = 6.4$  Hz), 4.05 (t, 2H,  $J = 6.6$  Hz), 1.22–1.86 (m, 33H), 0.85–0.91 (m, 6H),  $\delta_C$  (CDCl<sub>3</sub>) 165.54, 164.47, 163.75, 154.64, 132.39, 131.09, 128.36, 121.75, 121.08, 114.37, 71.90, 68.38, 36.08, 31.93, 31.75, 29.65, 29.60, 29.57, 29.36, 29.16, 29.09, 25.98, 25.41, 22.70, 22.60, 20.10, 14.13, 14.07.

## Results

### Variation of the chiral terminal group

Anticlinic/antiferroelectric order is readily obtained if 1-methylalkyl is used as one of the terminal chains. Similarly as for MnPOBC<sup>8</sup> or MnOMBB<sup>9</sup> (1-methylalkanyl 4-[(4'-alkoxy-4-oxymethyl)biphenyl]benzoate) analogous series having carboxy and methoxy linkages between the biphenyl and phenyl units in the mesogenic core, respectively, in the studied homologous series the appearance of an antiferroelectric phase depends on the number of carbon atoms in the chiral alkyl chain, however it is not a simple odd–even effect (Table 1). For the studied compounds the range of the synclinc SmC\* phase, that appears above the antiferroelectric phase, is significantly broader (about 20 K) than for

**Table 1** The phase transition temperatures (in °C) and enthalpy changes (in J g<sup>-1</sup>) for the studied compounds

Compound	<i>n</i>	X	Y	Z	m.p.	SmC* <sub>A</sub>	SmC* <sub>Fi1</sub>	SmC*	SmA	Iso
<b>1</b>	2	H	H	H	74.0 (38.9)			•	118.2 (0.07)	•
<b>2</b>	3	H	H	H	69.6 (63.3)	•	96.9 (0.04)	•	116.5 (0.2)	•
<b>3</b>	5	H	H	H	68.2 (60.5)			•	113.4 (.3)	•
<b>4</b>	6	H	H	H	69.4 (54.9)	•	96.2 (0.01)	•	98.9 (0.02)	•
<b>5</b>	6	F	H	H	77.5 (59.8)	•	97.5 (0.04)	•	117.6 (0.5)	•
<b>6</b>	6	Cl	H	H	70.7 (28.9)			•	114.9 (0.75)	•
<b>7</b>	6	H	Cl	H	below 40			•	90.0 (0.3)	•
<b>8</b>	6	H	H	Cl	50.6 (28.8)			•	103.7 (5.6)	•
<b>9</b>	6	H	NO <sub>2</sub>	H	43.1 (29.6)			•	74. (7.6)	•
								•	65.4 (0.1)	•
								•	72.3 (0.1)	•
								•	85.8 (6.6)	•
								•	76.5 (5.9)	•

R	Phase sequence
<b>10</b> -CH(CH <sub>3</sub> )COOC <sub>2</sub> H <sub>5</sub>	Cry 70.6 (46.2) SmC* 107.4 (0.2) SmA 138.7 (6.0) Iso
<b>11</b> -PhCOOCH(CH <sub>3</sub> )C <sub>6</sub> H <sub>13</sub>	Cry 120.4 (44.0) SmC* 200.6 (0.3) SmA 227.4 (6.3) Iso
<b>12</b> bornyl	Cry 133.8 (67.0) SmC* 125.1 (0.7) SmA 140.9 (0.06) TGBA* 141.7 (0.2) N* 146.1 BP (0.06) BP 146.7 (0.01) BP 147.2 (1.7) Iso
<b>13</b> menthyl	Cry 114.7 (70.4) [SmA 90.1 (3.7)] Iso
<b>14</b> fenchyl	Cry 123.3 (66.5) Iso

MnPOBC and MnOMBB compounds. The spontaneous polarization increases with increasing chiral terminal chain length, from below 20 to above 100 nC cm<sup>-2</sup> (Fig. 1) for the shortest and longest homologues, respectively. This is a rather typical dependence, extending the terminal chain makes the zig-zag shape of the molecule<sup>10</sup> more pronounced,

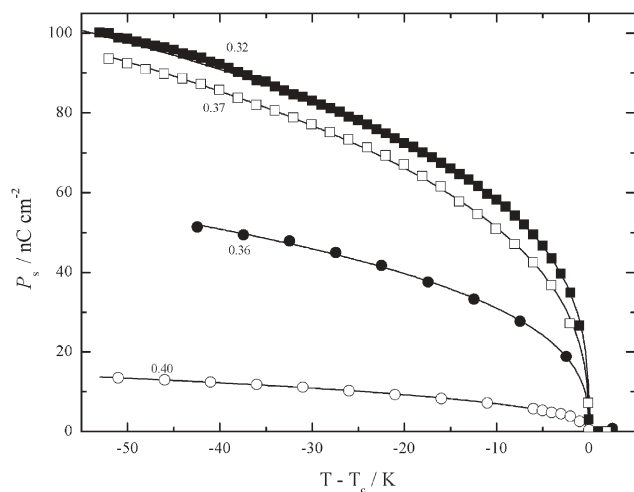


**Fig. 1** Spontaneous polarization *versus* temperature for homologous compounds **1** (open circles), **2** (solid circles), **3** (open squares) and **4** (solid squares). The lines are fits to power law,  $P_s \sim (T - T_c)^\beta$ , the critical exponents  $\beta$  are given on the curves.

which results in strongly hindered rotation around the long axis, thus stronger in-plane quadrupolar order.<sup>11</sup> There is no detectable anomaly in  $P_s$  value at the SmC\*–SmC\*<sub>A</sub> phase transition. The temperature dependence of  $P_s$  follows the power law,  $P_s \sim (T - T_c)^\beta$ , with critical exponents varying from 0.4 to 0.3, for the shortest and longest homologues, respectively. The angle at which the tilt saturates is ~30–35° for all homologues. The helical pitch gives a selective reflection in the SmC\* phase in the IR range for the shortest homologue and in the visible range for the longest homologue, while for the SmC\*<sub>A</sub> phase it always is in the visible range (Fig. 2). In both phases the pitch is only weakly temperature dependent. The sign of the pitch reverses on going from the ferro to the antiferro phase.

Detailed studies were performed for longest homologue, **4**, for which the ferroelectric SmC\*<sub>Fi1</sub> phase was additionally observed between the SmC\* and SmC\*<sub>A</sub> phases. This particular compound was synthesized previously by Nguyen *et al.* (designated by the acronym 12HHBMM7) and was described as having two ferroelectric mesophases with identical electrooptic properties.<sup>12</sup> In our studies, however, we do not see evidence for the additional phase transitions. In the temperature range between the SmC\* and SmC\*<sub>A</sub> phases, in DSC measurements, only SmC\*–SmC\*<sub>Fi1</sub> and SmC\*<sub>Fi1</sub>–SmC\*<sub>A</sub> phase transitions could be resolved on slow cooling and heating runs. The proposed phase sequence is also consistent with the optical and dielectric studies described below.

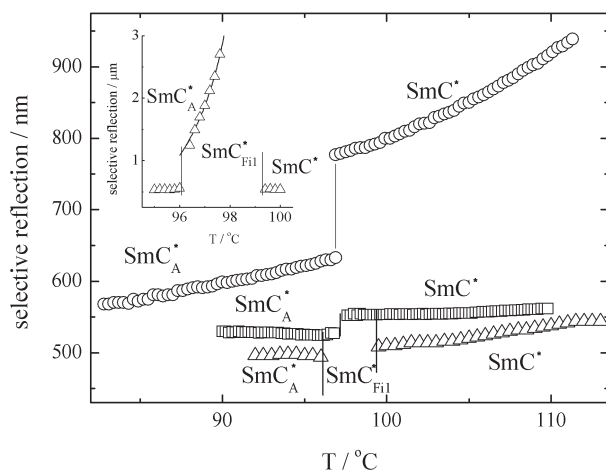


**Fig. 2** Selective reflection wavelength obtained for normal light incidence for thick ( $\sim 100 \mu\text{m}$ ) free standing film samples of compounds **2** (circles) and **4** (triangles) and fluorinated compound **5** (squares). In the inset is shown the selective reflection wavelength measured in  $\text{SmC}^*_{\text{F11}}$  of compound **4**.

In compound **4** the helical structure of the  $\text{SmC}^*$  and  $\text{SmC}^*_\text{A}$  phases gives rise to selective light reflection in the visible light range nearly of the same wavelength, while the sign of the helix is reversed as evidenced by the reversed sign of the ORP (Fig. 3). The helical pitch in  $\text{SmC}^*_{\text{F11}}$  is considerably longer and strongly temperature dependent. However, in the narrow, about 1 K, temperature range of the  $\text{SmC}^*_{\text{F11}}$  phase above the  $\text{SmC}^*_\text{A}$  phase, selective reflection could be still detected by spectroscopic methods. As the temperature increases, the helix unwinds and rewinds with opposite handedness. The inversion temperature  $T_i$  is  $\sim 2$  K above the transition from the  $\text{SmC}^*_\text{A}$  phase. The temperature dependence of the ORP follows the pitch temperature dependence (Fig. 3). In the  $\text{SmC}^*_{\text{F11}}$  phase it increases in magnitude on heating towards  $T_i$ , becomes out of the measurable range in

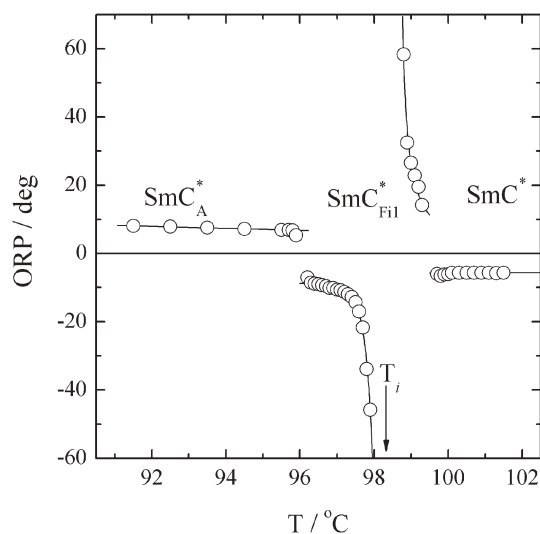


**Fig. 3** Optical rotatory power vs. temperature for compound **4** measured for a free standing film sample of thickness  $\sim 50 \mu\text{m}$ . The arrow indicates the helix twist inversion temperature.

the vicinity of the unwinding, and reappears with the opposite sign above  $T_i$ . We conclude that for the *R*-enantiomer of **4** there is a right-handed helix in the  $\text{SmC}^*_\text{A}$  phase, right-handed reversing to left-handed in the  $\text{SmC}^*_{\text{F11}}$  phase upon increasing temperature, and a left-handed helix in the  $\text{SmC}^*$  phase. Studies of the free-standing film samples around the unwinding temperature enable observation of the director field, since around  $T_i$  the averaging of the optical dielectric tensor due to the helical superstructure is absent. Around temperature  $T_i$  the birefringent Schlieren-type texture with numerous disclination defects was observed and the non-zero birefringence evidences the distortion from the perfect clock structure of the crystallographic unit cell (Fig. 4). The perfect clock structure, due to the averaging effect in the three layer unit, should give zero birefringence for the light propagating along the layer normal and the maximum birefringence should be observed for the perfect Ising *i.e.* all-in-one-plane structure. According to the de Vries formula<sup>13</sup> ORP is a function of helical pitch ( $p$ ) and in-plane dielectric anisotropy ( $\Delta\epsilon$ ):

$$\text{ORP} = \frac{2\pi}{p} \left( \frac{\Delta\epsilon}{\bar{\epsilon}} \right)^2 (8\lambda^2(1-\lambda^2))^{-1}$$

with  $\lambda = \lambda_0 n p$ ,  $\lambda_0$  is the wavelength of the light,  $\bar{\epsilon}$  is the mean dielectric tensor, and  $n$  the mean refractive index. Knowing the change of ORP and helical pitch between the  $\text{SmC}^*_\text{A}$  and  $\text{SmC}^*_{\text{F11}}$  phases the change in the in-plane dielectric anisotropy for the light propagating parallel to the layer normal could be obtained.

$$\Delta\epsilon_{\text{F11}} / \Delta\epsilon_{\text{CA}} = \frac{1}{3} (4 \cos^2(\alpha/2) - 1)$$

This change is due to the distortion from the all-in-one-plane ( $\alpha = 0$ ) structure. For the studied system it was found that  $\Delta\epsilon_{\text{F11}}/\Delta\epsilon_{\text{CA}} \sim 1 \pm 0.02$ . This gives an azimuthal angle  $\alpha$  that is not bigger than 14 degrees, and constant within the temperature range of  $\sim 1$  K above the  $\text{SmC}^*_\text{A}$ – $\text{SmC}^*_{\text{F11}}$  phase transition, where reliable data for helical pitch could be obtained. Our preliminary studies show that for the studied system the  $\alpha$  angle is temperature independent but might depend essentially on the enantiomeric purity of the material. The change of dielectric anisotropy between  $\text{SmC}^*$  and  $\text{SmC}^*_\text{A}$  phases for the studied compound, calculated from ORP measurements, is  $\Delta\epsilon_{\text{C}}/\Delta\epsilon_{\text{CA}} \sim 0.91 \pm 0.03$ , that is slightly different than 1 due to a small decrease of the tilt angle magnitude, which decreases the in-plane dielectric anisotropy in the  $\text{SmC}^*$  phase.

The dielectric response in the  $\text{SmC}^*_\text{A}$  phase shows a single, weak relaxation mode (Fig. 5) that has an Arrhenius type temperature dependence  $f_r = f_0 \exp(-E_a/T)$  with activation

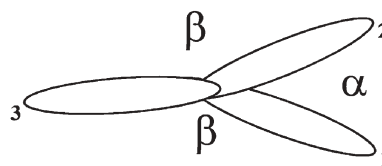


**Fig. 4** Three layer basic structural unit of the  $\text{SmC}^*_{\text{F11}}$  phase (viewed along the layer normal). Azimuthal angles  $\alpha$  and  $\beta$  different than  $120^\circ$  define the distortion from the perfect clock-like structure.

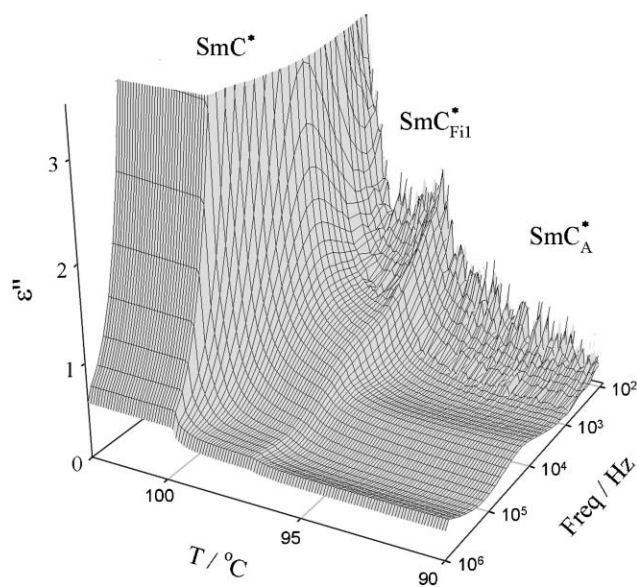


**Fig. 5** Imaginary part of dielectric constant vs. temperature and frequency for compound **4** in the temperature range of the  $\text{SmC}^*_{\text{F11}}$  phase.

energy  $E_a = 98 \text{ kJ mol}^{-1}$ . This mode is probably related to the distortion of the antiferroelectric, two layer structure of the crystallographic unit cell.<sup>14</sup> The crystallographic unit cell distortion dielectric mode is also observed in the  $\text{SmC}^*_{\text{F11}}$  phase. Additionally, in the  $\text{SmC}^*_{\text{F11}}$  phase a low frequency mode is present; however its frequency could not be determined precisely. The attempts to fit the dielectric data with a Cole–Cole dependence indicate that the mode relaxation frequency is in the range 1–100 Hz and the mode has a large distribution parameter (0.2–0.3). The presence of this mode, with strength significantly lower than in the  $\text{SmC}^*$  phase, shows that polarization is partially compensated in the three layer crystallographic unit cell of the  $\text{SmC}^*_{\text{F11}}$  phase,

which is consistent with optical measurements. The distortion of the long wavelength helix is probably the main contribution to the mode, but its polydispersed nature shows that other relaxation mechanisms are also present in the same frequency window, for example movements of the defect walls formed at the boundaries of the domains with opposite directions of  $P_s$  and  $-P_s$  in crystallographic units.<sup>5</sup>

In all studied compounds having  $\text{SmC}^*$  and  $\text{SmC}^*_A$  phases strong hysteresis of the dielectric response is observed in the  $\text{SmC}^*$  phase (Fig. 6). In this phase, on cooling, the helix distortion (so called goldstone) mode is nearly temperature independent. However, on heating from the  $\text{SmC}^*_A$  phase (directly or through the  $\text{SmC}^*_{\text{F11}}$  phase) the dielectric response is much stronger and has lower relaxation frequency that observed in the cooling scan. On further heating, a few degrees above the transition to the  $\text{SmC}^*$  phase the dielectric mode strength suddenly decreases and its relaxation frequency increases. These changes are correlated with the sample texture changes. In the temperature range of stronger dielectric response the helical pitch, judged from the periodicity of disclination lines observed in the planar cell, so-called dechiralization lines,<sup>15</sup> is in the micrometer range and suddenly decreases at the temperature where the dielectric response decreases. The effect was confirmed in samples of various thickness (from 5 to 100  $\mu\text{m}$ ) and for different electrode layers (ITO or gold). Since measurements of helical pitch by spectroscopic methods in free suspended film samples do not show any anomaly in this temperature range (see Fig. 2), the effect is clearly related to surface interactions.

Other compounds with cyclic chiral terminal groups:<sup>16</sup> fenchyl (**14**) and menthyl (**13**) units, did not show liquid crystalline properties or exhibited only a monotropic mesophase (Table 1). However, for compound **12** with a bornyl unit, a broad range of liquid crystalline phases with complex polymorphism Iso–BP–N\*–TGBA\*–SmA–SmC\* is observed. The helical pitch in the N\* and  $\text{SmC}^*$  phases is short, giving

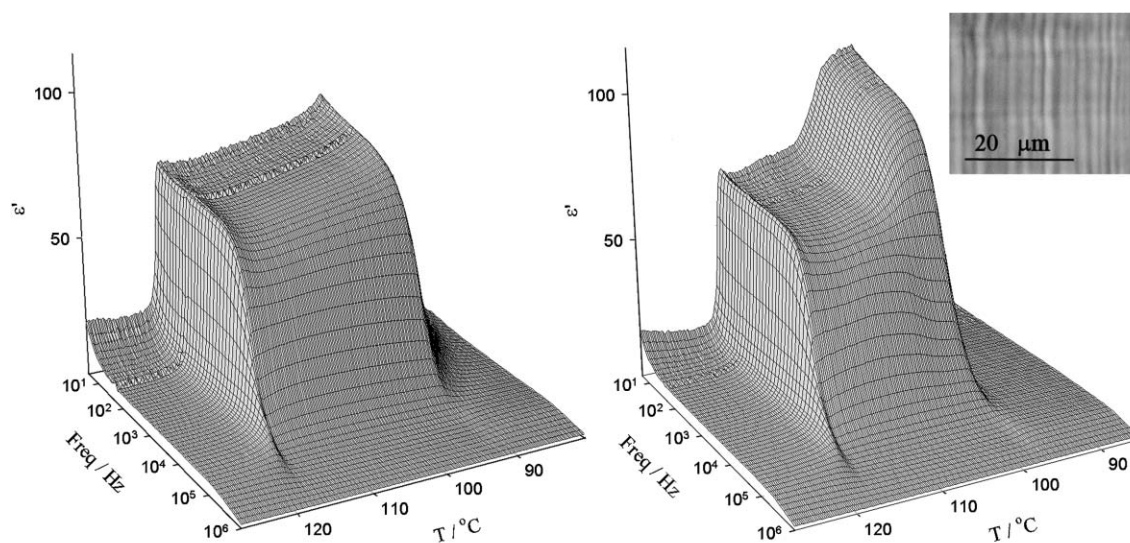


**Fig. 6** Dielectric dispersion vs. temperature for compound **4** taken in cooling (left) and heating (right) scans, in a 6  $\mu\text{m}$  thick glass cell with ITO electrodes. The sudden change in the relaxation process observed in the heating scan is correlated with texture changes. In the inset is shown the texture with dechiralization lines observed on heating at 103  $^\circ\text{C}$ .

selective reflection in the UV range; in the TGBA\* phase it is in the visible range. The spontaneous polarization in the SmC\* phase is below  $30 \text{ nC cm}^{-2}$ .

For the material **10** with a lactic acid end group only SmA and ferroelectric SmC\* phases are observed showing that this terminal chain has lower induction ability for anticlinic order than a 2-methylalkyl chain.

### Variation of the mesogenic core

Introducing the lateral substituent to the mesogenic core suppresses the range of liquid crystalline phases, as the substituent increases the width to length ratio. In all materials only synclinc order is observed, except for the smallest fluorine substituent (compound **5**) for which also the anticlinic phase was detected. It is interesting to note that the position of the lateral group in the mesogenic core influences the ferroelectric properties profoundly. If the chlorine atom is attached to the phenyl ring most distant from the chiral centre (compound **6**), the polarization is only slightly decreased compared to the non-substituted compound ( $P_s = 78 \text{ nC cm}^{-2}$ , 30 K below the SmA–SmC\* phase transition). If the chlorine atom is substituted at the phenyl ring closest to the chiral centre (compound **8**) the polarization strongly decreases ( $P_s = 45 \text{ nC cm}^{-2}$ , 30 K below the SmA–SmC\* phase transition). In this case, apparently the dipole moment of the carbonyl group (the one close to the chiral centre), which is to a great extent responsible for the spontaneous polarization,<sup>17</sup> is diminished in the presence of the nearby electron-accepting chlorine substituent. If the chlorine atom is substituted at the intermediate phenyl ring (compound **7**) only an orthogonal SmA phase is observed. However, if the chlorine group is exchanged for an NO<sub>2</sub> substituent (compound **9**) the SmA phase is strongly suppressed and a ferroelectric SmC\* phase again is observed, with spontaneous polarization even higher than for material **4** ( $P_s = 100 \text{ nC cm}^{-2}$ , 30 K below the SmA–SmC\* phase transition).

Extending the mesogenic core by an additional benzyloxy-carbonyl unit (compound **11**) raises the clearing temperature by about 100 K and only a synclinc tilted phase is observed. The spontaneous polarization, up to  $70 \text{ nC cm}^{-2}$ , is lower than for analogous three ring compound **4**.

### Discussion

Results of our studies show that attaching a 2-methylalkyl chain to a mesogenic core made of repeating benzyloxy-carbonyl units gives compounds able to form synclinc and anticlinic phases. However, the interactions leading to synclinc structure are for the studied materials apparently stronger than for the parent MnPOBC or MnOMBB compounds as evidenced by the much broader range of the synclinc phase and less frequent appearance of anticlinic phases in the homologous series. The ferroelectric SmC\*<sub>Fil</sub> phase that is usually observed between the SmC\* and SmC\*<sub>A</sub> phases for materials with a narrow temperature range of the SmC\* phase, in the studied series is observed only for compound **4** with the longest chiral alkyl chain, below the broad range of the SmC\* phase. The ferroelectric phase has a nearly Ising structure ( $\alpha < 14^\circ$ ), for comparison in MHPOBC

$\alpha \sim 40\text{--}45^\circ$ ,<sup>5,18</sup> in 100TBBB1M7  $\alpha \sim 45\text{--}50^\circ$ ,<sup>5,18</sup> and for MHPBC  $\alpha \sim 36^\circ$ <sup>19</sup> was found by optical methods. The difference is probably due to the range of the SmC\* phase that precedes the SmC\*<sub>Fil</sub> phase, in the studied system the SmC\*<sub>Fil</sub> phase appears  $\sim 20 \text{ K}$  below the SmA–SmC\* phase transition. This indicates that quadrupole interlayer interactions, that tend to keep molecules in the same tilt plane, might indeed play an important role in the distortion of the clock-like structure. It is reasonable to expect that these interactions grow with lowering temperature and become considerable in materials with a broad range of the SmC\* phase.<sup>20</sup>

In studied material **4** for the first time a helix twist inversion within the temperature range of the SmC\*<sub>Fil</sub> phase was observed. The long wavelength helical modulation is a result of the small incommensurability of the three layer structure.<sup>6</sup> In the SmC\*<sub>Fil</sub> phase the azimuthal angle changes in consecutive layers as  $\alpha, \beta, \beta$  with  $\alpha + 2\beta$  slightly different from  $2\pi$ . The helix inversion occurs at the temperature at which the structure becomes exactly commensurate, with  $\alpha + 2\beta = 2\pi$ . It should be stressed that the basic three layer structural unit does not change at the optical helix reversing temperature. This shows that there is no simple relation between the molecular chirality, chirality of the crystallographic unit cell and long wavelength helical modulations.

For the broad range of the SmC\* phase, above the SmC\*<sub>A</sub> phase strong hysteresis of the dielectric response for heating and cooling scans was detected. The effect is clearly related to surface interactions. It is reasonable to assume that upon heating into the SmC\* phase, from the SmC\*<sub>A</sub> phase, the surface layers remain anticlinic/antiferroelectric, while the bulk is ferroelectric. It is observed that such geometry leads to the helix unwinding, the helical pitch is much longer than its equilibrium value, found in surface free samples. Above a certain temperature apparently the surface layer undergoes a transition into a synclinc/ferroelectric state and the change in the surface layer allows the formation of a helix with shorter, close to equilibrium pitch. Since the dielectric response is related to the periodicity of helical modulations in the cell, the change in the pitch corresponds to the sudden change in the dielectric response within the SmC\* phase temperature range.

### Acknowledgements

This work was supported by the KBN grant 4T09A 00425.

**Ewa Dzik, Józef Mieczkowski,\* Ewa Gorecka and Damian Pocięcha**  
 Warsaw University, Department of Chemistry, ul. Pasteura 1, 02-093,  
 Warsaw, Poland. E-mail: mieczkow@chem.uw.edu.pl;  
 Fax: +48 22 8221075; Tel: +48 22 8221075

### References

- 1 A. D. L. Chandani, E. Gorecka, Y. Ouchi, H. Takezoe and A. Fukuda, *Jpn. J. Appl. Phys.*, 1989, **28**, L1265; E. Gorecka, A. D. L. Chandani, Y. Ouchi, H. Takezoe and A. Fukuda, *Jpn. J. Appl. Phys.*, 1990, **29**, 131.
- 2 A. Fukuda, Y. Takanishi, T. Isozaki, K. Ishikawa and H. Takezoe, *J. Mater. Chem.*, 1999, **9**, 2051 and references therein.
- 3 E. Gorecka, D. Pocięcha, M. Cepic, B. Zeks and R. Dąbrowski, *Phys. Rev. E*, 2002, **65**, 61703.
- 4 P. Mach, R. Pindak, A. M. Levelut, P. Barois, H. T. Nguyen, C. C. Huang and L. Furenlid, *Phys. Rev. Lett.*, 1998, **81**, 1015;

- P. Mach, R. Pindak, A. M. Levelut, P. Barois, H. T. Nguyen, H. Baltes, M. Hird, K. Toyne, A. Seed, J. W. Goodby, C. C. Huang and L. Furenlid, *Phys. Rev. E*, 1999, **60**, 6793; A. Cady, J. A. Pitney, R. Pindak, L. S. Matkin, S. J. Watson, H. F. Gleeson, P. Cluzeau, P. Barois, A. M. Levelut, W. Caliebe, J. W. Goodby, M. Hird and C. C. Huang, *Phys. Rev. E*, 2001, **64**, 50702; L. S. Hirst, S. J. Watson, H. F. Gleeson, P. Cluzeau, P. Barois, R. Pindak, J. Pitney, A. Cady, P. M. Johnson, C. C. Huang, A. M. Levelut, G. Srajer, J. Pollmann, W. Caliebe, A. Seed, M. R. Herbert, J. W. Goodby and M. Hird, *Phys. Rev. E*, 2002, **65**, 41705; L. S. Matkin, H. F. Gleeson, L. J. Baylis, S. J. Watson, N. Bowring, A. Seed, M. Hird and J. W. Goodby, *Appl. Phys. Lett.*, 2000, **77**, 340.
- 5 M. Cepic, E. Gorecka, D. Pocięcha, B. Žeks and H. T. Nguyen, *J. Chem. Phys.*, 2002, **117**, 1817.
- 6 M. B. Hamaneh and P. L. Taylor, *Phys. Rev. Lett.*, 2004, **93**, 67801.
- 7 K. Yoshino, H. Taniguchi and M. Ozaki, *Ferroelectrics*, 1989, **91**, 267; K. Fujisawa, C. Sekine, Y. Uemura, T. Higashii, M. Minai and I. Dohgane, *Ferroelectrics*, 1991, **121**, 167.
- 8 J. Thisayukta and E. T. Samulski, *J. Mater. Chem.*, 2004, **14**, 1554.
- 9 J. Szydłowska, D. Pocięcha, E. Gorecka, D. Kardas, J. Mieczkowski and J. Przedmojski, *J. Mater. Chem.*, 1999, **9**, 361. Materials described there will be referred to by the acronym MnOMBB.
- 10 R. Bartolino, J. Doucet and G. Durand, *Ann. Phys. (Paris)*, 1978, **3**, 389; D. Guillon and A. Skoulios, *J. Phys. (Paris)*, 1977, **38**, 79.
- 11 H. F. Gleeson, Y. Wang, S. Watson, D. Sahagun-Sanchez, J. W. Goodby, M. Hird, A. Petrenko and M. A. Osipow, *J. Mater. Chem.*, 2004, **14**, 1480.
- 12 V. Faye, J. C. Rouillon, C. Destrade and H. T. Nguyen, *Liq. Cryst.*, 1995, **19**, 47; J. W. O'Sullivan, J. K. Vij and H. T. Nguyen, *Liq. Cryst.*, 1997, **23**, 77; F. Bibonne, J. P. Parneix and H. T. Nguyen, *Eur. Phys. J. Appl. Phys.*, 1998, **3**, 237.
- 13 H. P. de Vries, *Acta Crystallogr.*, 1951, **4**, 219.
- 14 N. Vaupotic, M. Cepic and B. Žeks, *Ferroelectrics*, 2000, **245**, 175.
- 15 M. Brunet and C. Williams, *Ann. Phys.*, 1978, **3**, 137; M. Glogarova, L. Lejcek, J. Pavel, U. Janovec and F. Fousek, *Mol. Cryst. Liq. Cryst.*, 1983, **91**, 309.
- 16 J. Mieczkowski, E. Gorecka, D. Pocięcha and M. Glogarova, *Ferroelectrics*, 1998, **212**, 357.
- 17 A. Terzis, D. Photinos and E. Samulski, *J. Chem. Phys.*, 1997, **107**, 4061.
- 18 I. Musevic and M. Skarabot, *Phys. Rev. E*, 2001, **64**, 51706.
- 19 P. M. Johnson, D. A. Olson, S. Pankratz, H. T. Nguyen, J. Goodby, M. Hird and C. C. Huang, *Phys. Rev. Lett.*, 2000, **84**, 4870.
- 20 D. Pocięcha, E. Gorecka, M. Cepic, N. Vaupotic, B. Žeks, D. Kardas and J. Mieczkowski, *Phys. Rev. Lett.*, 2001, **86**, 3048.